

Analysis of Polygon Taper Shank and Spindle Contact State Simulation

Zhigang Wang^a Jing Wang^b and Zhenhua Wu^c

Mechanical Engineering Department of Harbin University of Science and Technology

^awzghlmail@163.com, ^b15776768710@163.com, ^c15145086631@163.com

Abstract

According to the basic characteristics of the polygon taper shank connection type surface, analyzing the working principle of polygon type surface shank; based on the contact characteristics of polygon taper shank and spindle, establishing the torsional rigidity model of polygon taper shank, based on that, deriving the calculation formulas of contact force and magnitude of interference, and analyzing the equivalent stress of tapered surface and cylinder; using UG software to establish the three-dimensional model of polygon taper shank and spindle; making simulation on the stress condition of the shank and spindle by using the finite element analysis software ansys-workbench, obtaining the contact surface stress of shank and spindle under the clamping force, and providing theoretical basis for the using technology of shank.

Keywords: Polygon taper shank; Contact stress; Rigidity; Magnitude of interference; Simulation

1. Introduction

The traditional BT shank (7:24) has been unable to adapt to high speed machining because of its centrifugal force problem; while the HSK shank's taper 1:10 is small, the shank is similar to the straight shank, and what the contact of tapered surface and flange surface is required at the same time makes repairing and regrinding of the cutting tools difficult; polygon taper shank can realize transmission without the key because of its taper polyhedron structure, it has some advantages like large contact area, the low pressure on tool surface, the small wear, so it is used widely for high speed and high precision machine tool like turning machine tool centre and turning and milling tool centre, the contact state of shank and spindle has influence on not only quality of machined part and production efficiency, but also its own reliability and security, precision. In this paper, analyzing polygon taper shank and spindle joint, through the finite element method studying the contact state of the tapered surface and flange surface of shank and spindle joint in the static condition and under different clamping force, hoping to provide the help for the use and design of the shank.

2. The Working Principle of the Polygon Taper Shank and Spindle

Polygon taper shank becomes the international standard ISO-26623 in 2008. Shank joint structure, as shown in figure 1, is the taper 1:20 and three section of arc isometric type surface joint. Large torque is transmitted by the interaction of three curved surfaces AB, CD, EF. Using clamping way of the tapered surface and flange surface, as shown in figure 2^[4], eliminating axial positioning error. This kind of joint form has higher joint strength and higher centering precision than the joint of flat key and spline.

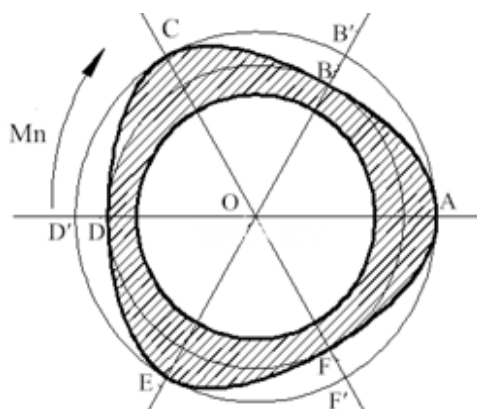


Figure 1. Section of Polygon Taper Shank

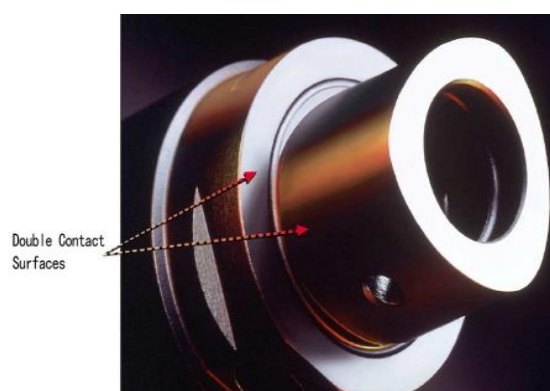


Figure 2. The Double Positioning Surface

3. Analysis And Calculation of Polygon Taper Shank and Spindle Joint Under Static Force

The joint of polygon taper shank and spindle hole belongs to the keyless joint and the polygon taper shank doesn't turn in the spindle hole. So all the passed torque acts on the shank's tapered surface. In order to analyze the contact characteristics, the main point of this chapter is the relevant mechanical formulas' derivation, including the contact pressure, torsional rigidity and magnitude of interference. They are the theoretical basis for the analysis of the back contact characteristic.

3.1. Torsional Rigidity of Polygon Taper Shank

According to the axial torsional rigidity in the mechanics of materials, torsional rigidity of the polygon taper shank is defined as: required torque that produces unit torsion angle within the effective length direction of taper shank. As shown the torsional rigidity model in figure 3.

Torsional rigidity expression:

$$\phi = \frac{TL}{GI_{\rho}} = \frac{TL}{G(I_{\rho 1} + 3I_{\rho 2})} \quad (1)$$

Formula: G is shear elasticity modulus of material, I_r is the polar moment of inertia of polygon taper shank, and L is the length of shank tapered surface. so the expression of torsional rigidity:

$$C = \frac{GI_r}{L} = \frac{G(I_{r1} + 3I_{r2})}{L} \quad (2)$$

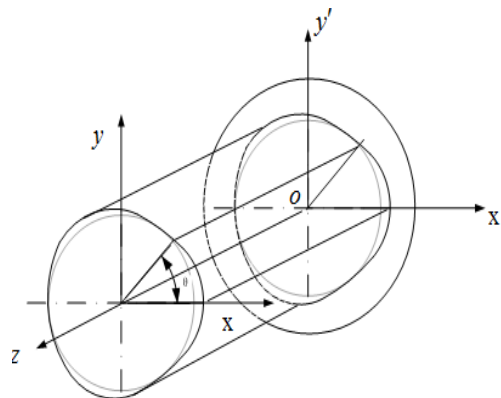


Figure 3. Shank Twisting Model

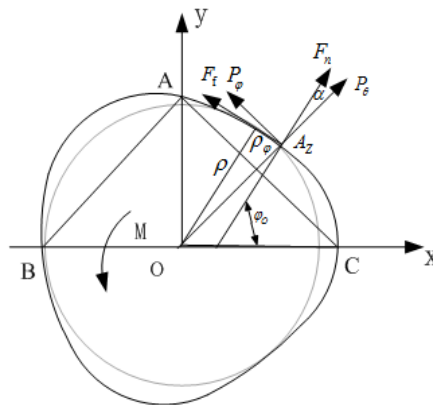


Figure 4. Calculation of Contact Pressure

3.2. The Contact Pressure of Shank and Spindle Joint

For the calculation of the shank and spindle contact pressure, based on elastic theory, engineering calculation method is as shown in figure 4. Through the geometric relationships as shown in figure 4, the angle between contact pressure and the polar diameter of the A is α , so

$$\begin{cases} \tan \alpha = \frac{nm \sin 2\varphi - 2m \sin \varphi - 2 \cos \varphi - n \cos 2\varphi}{\rho} \\ \sin \alpha = \frac{n \sin 2\varphi - 2 \sin \varphi + 2m \cos \varphi + mn \cos 2\varphi}{\rho} \end{cases} \quad (3)$$

Assuming that the length of the tapered surface that is fitted with the spindle is l , friction coefficient is f . We get the torque of the total force on the micro area d_s to axis O,

$$dM = pdFn \sin \alpha \rho + pdF_f \rho(\varphi) \quad (4)$$

Due to the symmetry of shank section, calculating torque in a contact area in formula 7, and the total torque is $3dM$. so,

$$M = 3lp \int_0^{\pi} [3n \sin 3\varphi + f(r + n \cos N\varphi)] \cdot (r - 8n \cos 3\varphi) d\varphi \quad (5)$$

So the calculation formula of contact pressure,

$$q = \frac{M}{l \left[3Dn + \pi fD^2/4 \right]} \quad (6)$$

3.3. Calculation of Magnitude of Interference of Polygon Taper Shank and Spindle

According of the ISO-26623, the taper angle of shank is $\theta_1 = 1^\circ 26' 21'' \pm 25''$, the taper angle of spindle hole is $\theta_2 = 1^\circ 25' 31'' \pm 25''$, producing maximum and minimum magnitude of interference by the change of taper, as shown in table 1, 2.

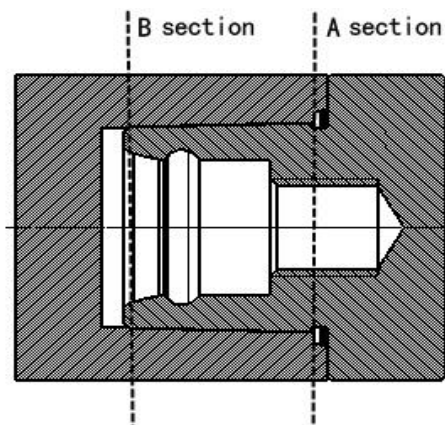


Figure 5. Shank and Spindle Assembly Section View

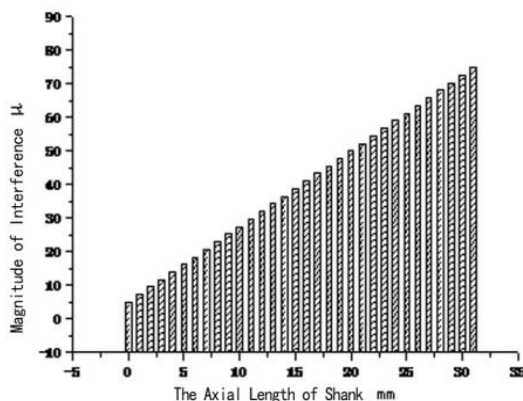


Figure 6. Magnitude of Interference along the Taper Axial

Large end size of polygon taper shank and the size of the spindle are basically same here, without considering the tolerance, controlling the magnitude of interference by the axial displacement and the change of spindle taper angle. Therefore, the large end to end of magnitude of interference increases along the axial, the large end of the maximum magnitude of interference is 5μ , the small end of maximum magnitude of interference can be up to 75μ , as shown in figure 6. The average value of A and B section magnitude of the interference is $\Delta_{\text{平均}} = (\Delta_A + \Delta_B) / 2$, used as the shank of magnitude of interference, the average maximum magnitude of interference of polygon taper shank and spindle is Δ

$\Delta_{\max}=40 \mu$, the average minimum interference is $\Delta_{\min}=32 \mu$.

Table 1. A Cross-Sectional Maximum Magnitude of Interference

	Taper angle	Max magnitude of interference taper angle(°)	A section radius (mm)	B Section radius (mm)
shank	1°26'21"±25"	1.4322	22.000	21.162
spindle	1°25'31"±25"	1.4322	21.995	21.087
Max magnitude of interference			0.005	0.075

Table 2. A Cross-Section Minimum Magnitude of Interference

	Taper angle	Min magnitude of interference taper angle(°)	A section radius (mm)	B Section radius (mm)
shank	1°25'31"±25"	1.4461	22.000	21.1569
spindle	1°26'21"±25"	1.4183	21.995	21.0963
Min magnitude of interference			0.005	0.0606

4. Static Simulation Analysis of Contact

4.1. Establishing the Shank and the Spindle Finite Element Contact Model

Based on the UG, establishing directly model of the polygon taper shank and spindle, as shown in figure 7. Then selecting hexahedron meshing method to analyze the assembly, as shown in figure 8 [7].

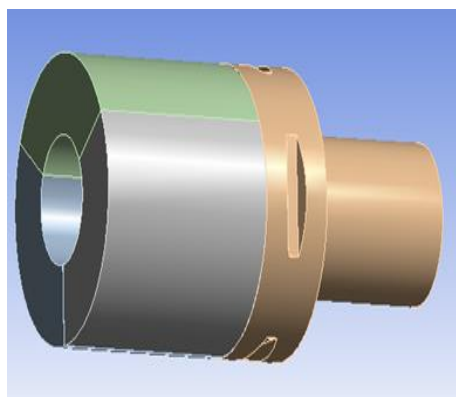


Figure 7. Polygon Shank and Spindle Assembly Model

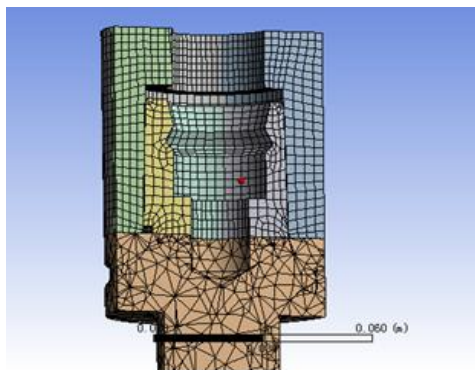


Figure 8. Internal Meshing of Polygon Shank

4.2. Influence of Clamping Force On the Taper Surface Contact Pressure

Clamping force decides the shank contact pressure in the static. As shown in figures 9, 10, it's about contact pressure distribution under different clamping force: the contact pressure of shank is more evenly on the large end surface along the z axis from 0mm to 15mm. With the increase of clamping force, the pressure decreases rapidly 25mm-30mm far away from x axis, but the pressure increases rapidly 30mm~35mm far away from x axis. Overall case, contact pressure distribution of shank is more uniform and the contact area is larger. In addition, the contact pressure value of large end and end has little difference. So shank has less concentrated pressure [8].

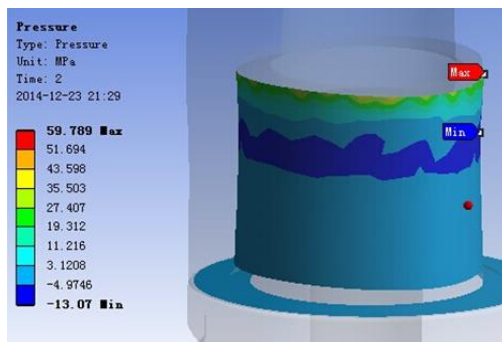


Figure 9. Contact Pressure Image of Spindle and Shank

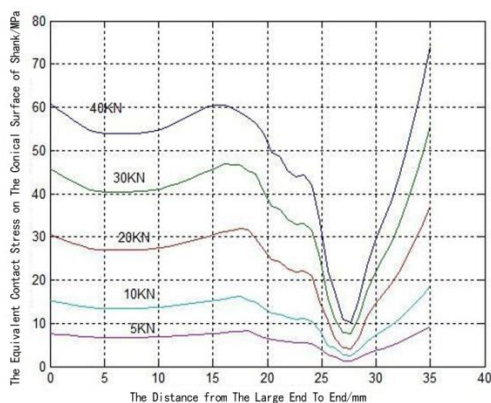


Figure 10. Equivalent Contact Stress under Different Clamping Force

4.3. Influence of Clamping Force on the End Contact Pressure

The contact surface determines the shank axial positioning accuracy and the axial rigidity. Fixing the magnitude of interference between the shank and spindle tapered surface, studying the shank flange surface contact pressure under the different clamping forces.

Figure 11 shows the spindle end face contact pressure images under the different clamping forces. It can be seen when the clamping force increases with 5KN, 10KN, 20KN, 30KN, 40KN, the end face contact pressure increases gradually and pressure distribution is uneven. From the end face inner diameter to the outer edges, the equivalent stress decreases gradually, the shank contact pressure along the radial direction of the end decreases and then increases, it is the highest near the taper shank. The reason is that when the spindle speed is zero or low speed, under the tensioning force, the axial movement of the shank leads to the extrusion between the tapered surface and the spindle hole, which causes the spindle hole expansion. According to image, the largest volume expansion of the end of spindle tapered hole leads to the end lateral warping, the contact pressure is larger near the intersection of shank flange surface and the tapered surface. On the other hand, under the tension of the tie rod, the shank passes the tension to end which will force the flange surface protruding deformation to the tension direction, coupled with the stress concentration at the junction of the tapered surface and end, it appears the trend that contact pressure is small in the middle and large near the taper shank. Such as shown in figure 12, it can be seen that tension increase as 10KN gradually and the increasing tendency of end contact pressure is more and more obvious, 40KN causes the shank end contact pressure unevenness along the radial too much. The appropriate tension range should be between 20KN to 30KN [9].

4.4. Equivalent Stress Analysis of Tapered Surface and Cylinder

When the tension force is 30KN and the speed is zero, the equivalent stress image of tapered surface and cylinder is as shown in figure 13. It is obvious that equivalent stress of

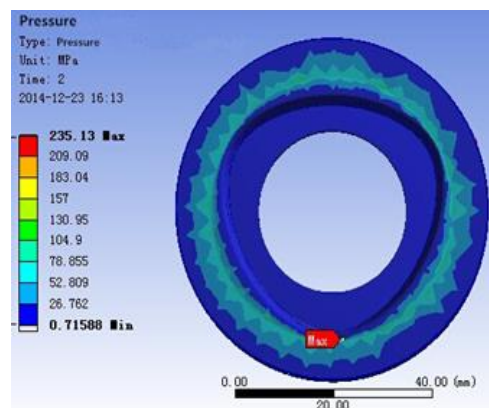


Figure 11. Contact Pressure Image of Spindle and Shank

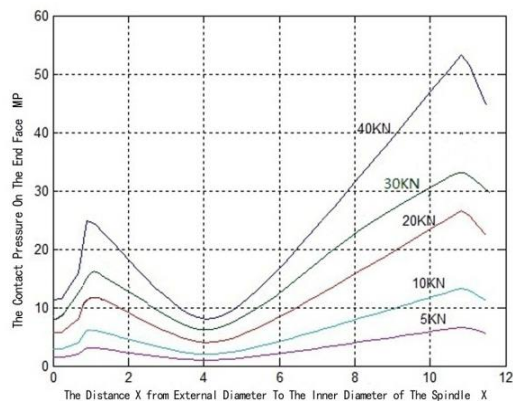


Figure 12. Contact Pressure of End Face under Different Clamping Forces

Three edges of polygon taper shank is smaller than that of the non-edge. The main reason is: the three edges of the shank are thicker, which lead to the higher strength, taper shank produces elastic deformation under tension force, the deformation of three edges relative to the cylinder is smaller, so the equivalent stress is smaller. Observing the dynamic deformation of the shank, when loading the clamping force, the color of cylinder turns light first; when the equivalent stress of cylinder reaches a certain value that of three edges begins to increase obviously. Observing the equivalent stress curve as shown in figure 14 that of cylinder reduces obviously in 7mm of the small end, but that of the edges increases slightly. The shank produces elastic deformation due to the clamping force, especially the effect of clamping jaw, the small end of the shank expands outward like a horn mouth, appearing concave shape in the low-end of horn that is 7mm, where there is a gap between the shank and the spindle. According to the analysis of the curve, the edges play a positive role in the gap area.

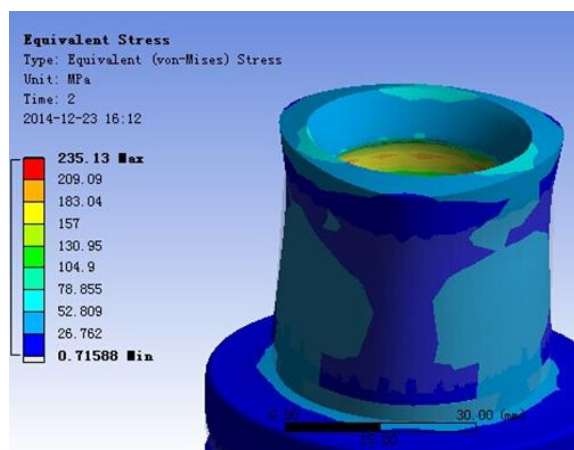


Figure 13. Equivalent Stress Image on Tapered Surface

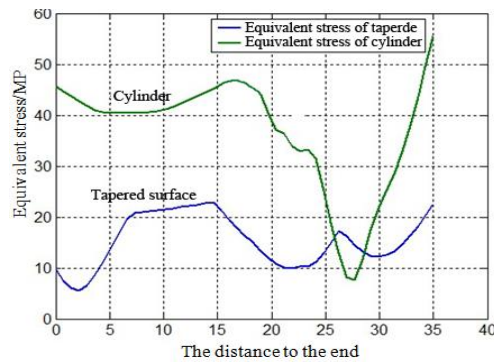


Figure 14. Equivalent Stress Curve of Tapered Surface and Cylinder

5. Conclusion

- (1) Only under the tensioning force, the equivalent stress of polygon taper shank edges is smaller than that of the cylinder, the edges play a positive role in the gap area.
- (2) We know that by simulation analysis of exerting different clamping forces on taper, overall, the contact pressure distribution of polygon taper shank taper is even. The contact area is larger. No obvious stress concentration.
- (3) Through the simulation analysis of the shank and spindle contact surface, we can know that when increasing the clamping force, the end contact pressure increases and the pressure distribution is uneven. Too much clamping force results in flange surface large deformation. The appropriate tension range should be between 20KN to 30KN.

References

- [1] W. Jie, G. Wang and C. Shen, "Reliability analysis of high speed spindle and shank interface. Mechanical design and manufacturing", no. 6, (2014).
- [2] Q. Cheng, X. Song and L. Cai, "Finite element analysis of the shank and spindle system coupling contact", Computer integrated manufacturing system, vol. 18, no. 4, (2012).
- [3] H. Xue, G. Wang and Z. Lu, "Research and development of tool system of high speed machining", Tool technology, vol. 40, no. 4, (2006).
- [4] X. Zhang (Compile), "Coromant Capto modular tool system", Tool outlook, no. 2, (2010).
- [5] Y. Zhou, C. Wang and Z. Qin, "The shank tool system in high speed machining", Mechanical design and manufacturing, no. 8, 2008.
- [6] Q. Jiang and J. Tao, "Connection mode and selection of high speed spindle and cutting tool of machining center", Journal of Anyang Institute of Technology, no. 4, (2012).
- [7] C. Liu, S. Wang, C. Shen and W. Chen, "Capto C6 spindle/toolholder interference characteristics of torsional stiffness", Modular machine tool and automatic manufacturing technique, no. 7, (2012).
- [8] H. Pen, X. Liu, Y. Wang, J. Hu, T. Chen and D. Liu, "Finite element simulation of cutting hardened bearing steel with high speed", Journal of Harbin University of Science and Technology, no. 2, (2007).
- [9] W. Liang, J. Hu, H. Pen, Y. Wang and X. Liu, "Finite element simulation of hard dry cutting process", Journal of Harbin University of Science and Technology, vol. 1, (2005).

